Available online at www.sciencedirect.com
SCIENCE DIRECT
Plant Science 169 (2005) 375–385
PLANT SCIENCE
www.elsevier.com/locate/plantsci

Cloning, functional analysis, and subcellular localization of two isoforms of NADH:cytochrome b_5 reductase from developing seeds of tung (*Vernicia fordii*)

Jay M. Shockey [a], Preetinder K. Dhanoa [b], Tammy Dupuy [c], Dorselyn C. Chapital [a], Robert T. Mullen [b], John M. Dyer [a,*]

[a] *Southern Regional Research Center, United States Department of Agriculture-Agricultural Research Service, 1100 Robert E. Lee Blvd., New Orleans, LA 70124, USA*
[b] *Department of Molecular and Cellular Biology, Room 302 Axelrod Building, 50 Stone Road East, University of Guelph, Guelph, Ont., Canada N1G 2W1*
[c] *Department of Biological Sciences, University of New Orleans, New Orleans, LA 70124, USA*

Received 31 January 2005; received in revised form 23 March 2005
Available online 25 April 2005

Abstract

Two genes and the corresponding cDNAs for NADH:cytochrome b_5 reductase (*VfCBR1A* and *VfCBR1B*) from tung (*Vernicia fordii*) were cloned and characterized. Both tung genes are expressed at similar levels in various organs throughout the plant, but differ substantially in their genomic architecture. Phylogenetic comparisons of many cloned and putative *CBR* genes from plants and yeast revealed two general classes of sequences. The separation of the classes likely reflects differences in the subcellular targeting of the two types of proteins. Immunofluorescence analyses of tobacco BY-2 cells containing transiently expressed tung CBR1A, CBR1B, or *Arabidopsis thaliana* CBR revealed definitive targeting of the proteins to the endoplasmic reticulum while a previously uncharacterized Arabidopsis CBR protein was targeted specifically to mitochondria. After overexpression in *Saccharomyces cerevisiae*, VfCBR1A was enzymatically active, and like its Arabidopsis ortholog, displayed strict specificity for NADH as the reductant. The subcellular localization and biochemical properties of the tung enzymes are consistent with a potential role in fatty acid desaturation and conjugation.

Keywords: *Vernicia fordii*; Tung; NADH cytochrome b_5 reductase; *Arabidopsis thaliana*; Endoplasmic reticulum; Mitochondria

1. Introduction

The seed oils of many non-domesticated plant species contain high amounts of industrially important fatty acids (e.g. hydroxy, epoxy, conjugated, and acetylenic), and there is significant interest in transferring genes required for the production of these fatty acids to organisms that have robust agronomic traits [1]. In recent years, genes responsible for the synthesis of these fatty acids have been identified, and in many cases have been shown to be diverged forms of the delta-12 fatty acid desaturase (FAD2) enzyme [2]. Expression of these diverged FAD2 genes in transgenic plants, however, has routinely resulted in much lower accumulation of the desired fatty acid than is observed in the source plant, indicating that additional genes from the source plant will be required to increase productivity [3].

The FAD2 and diverged FAD2 enzymes are membrane-bound proteins located in the endoplasmic reticulum (ER) that act upon fatty acyl substrates bound to phosphatidylcholine [2]. During the catalytic cycle of FAD2, two hydrogen atoms are extracted from the fatty acid substrate and transferred to an oxygen atom to produce water as a byproduct. This reduction of oxygen also requires a pair of electrons, which are provided by the microsomal electron transport chain composed of NADH:cytochrome b_5 reduc-

* Corresponding author. Tel.: +1 504 286 4351; fax: +1 504 286 4419.
E-mail address: jdyer@srrc.ars.usda.gov (J.M. Dyer).

0168-9452/$ – see front matter © 2005 Elsevier Ireland Ltd. All rights reserved.
doi:10.1016/j.plantsci.2005.03.023

tase (CBR, EC 1.6.2.2) and cytochrome b_5. For diverged FAD2 enzymes, subtle differences in the active site of the enzymes alter the substrate/product relationships, resulting the formation of hydroxy, epoxy, conjugated, and acetylenic fatty acids [2].

Our laboratory is interested in the production of conjugated fatty acids in the oils of transgenic plants. Conjugated fatty acids are more readily oxidized than typical polyunsaturated fatty acids, and therefore oils containing high amounts of these fatty acids have potential usage in the formulations of inks, dyes, coatings, and resins. We are studying the tung tree (*Vernicia fordii*) to identify genes for transgenic production of these oils. Seeds of the tung tree produce an oil that contains 80% α-eleostearic acid (9*cis*, 11*trans*, 13*trans* octadecatrienoic acid), an unusual conjugated fatty acid that imparts industrially useful drying qualities to tung oil. We previously identified all of the desaturases and diverged desaturase (conjugase) required for producing the polyunsaturated fatty acids in tung oil, including eleostearic acid [4,5], and more recently described the identification and functional analysis of four different cytochrome b_5 proteins from tung [6]. Interestingly, we found that three of these isoforms were targeted to the ER of plant cells, while the fourth was targeted specifically to the outer membrane of mitochondria.

Here we present the identification and characterization of two different *CBR* genes that are expressed in developing tung seeds during synthesis of tung oil. We describe the genomic architecture and organ-specific expression patterns of the genes, subcellular localization and enzymatic activity of the proteins, and compare these properties to two CBR proteins from Arabidopsis. Our results demonstrate that both of the tung CBR proteins and one of the Arabidopsis CBR proteins are targeted to the endoplasmic reticulum of plant cells, which is in agreement with the previously described microsomal location for the Arabidopsis enzyme [7]. The second Arabidopsis protein, however, was targeted specifically to mitochondria. Collectively, these results increase our understanding of *CBR* gene structure, expression, and protein biogenesis within plant cells. The availability of the tung *CBR* genes also provides tools for future attempts to enhance the production of eleostearic acid in the triacylglycerol fractions of transgenic plants [8].

2. Materials and methods

2.1. Sequencing and sequence homology analysis

All DNA constructs were sequenced using the DTCS Quickstart kit[1] (Beckman Coulter, Fullerton, CA) and analyzed on a Beckman Coulter 8800 Genetic Analysis System equipped with the CEQ8000 software suite. Sequences were manipulated and analyzed using VectorNTI Advance 9.0 software (InforMax, Invitrogen Life Science, Frederick, MD), and compared to other sequences using WWW-based BLAST algorithm programs [9]. Phylogenetic comparisons were carried out by generation of multiple sequence alignments using the CLUSTALX program, using the default settings. Dendograms were created from the alignments using the neighbor joining method [10] in the TreeView program [11].

2.2. Gene identification and cDNA cloning

Reverse strand degenerate primers were designed to the conserved amino acid sequence MSHHFREM spanning approximate amino acid residue positions 124–131 of the predicted protein sequences for Arabidopsis CBR [7], and maize NFRI [12] and NFRII [13]. Amplicons representing the putative 5′ ends of reductase cDNAs were generated by PCR amplification using the degenerate primers paired with the λ TriplEx 5′ LD-Insert Screening primer (5′-CTCGGG-AAGCGCGCCATTGTGTTGGT-3′). Phage lambda extract from the developing tung seed cDNA library [4] was used as the template. This library was prepared by Clontech Laboratories (BD Biosciences Clontech, Palo Alto, CA) from developing tung seed polyA RNA, and packaged into the vector pTriplEx. These products were gel-purified and cloned into the vector pCR2.1-TOPO (Invitrogen, Carlsbad CA). Upon verification of the 5′ ends by DNA sequencing, new gene-specific forward primers were designed and paired with the λ TriplEx 3′ LD-Insert Screening primer (5′-ATACGACTCACTATAGGGCG-3′) supplied in the kit to amplify the 3′ ends of the cDNAs. These products were cloned and sequenced as described earlier. Full-length open reading frames were amplified and cloned into pYES2.1-V5-His-TOPO (Invitrogen) for expression in *Saccharomyces cerevisiae*, or cloned into the pRTL2-myc vector [14] for plant cell bombardment and immunofluorescence studies. Full-length genes were amplified from tung genomic DNA and cloned into pCR2.1-TOPO (Invitrogen) for exon/intron structure determination.[2]

In addition to the cDNA clones described in this study, the CBR sequences representing cloned cDNAs used in the phylogenetic studies came from Arabidopsis (AtCBR1, called CBR by Fukuchi-Mizutani et al. [7]), maize [12,13], pumpkin [15], and *Saccharomyces cerevisiae* [16,17]. A putative second isoform of CBR from Arabidopsis (AtCBR2, At5g20080) was discovered by BLAST searches using AtCBR1 as a query sequence. All other sequences included do not come from cloned genes but instead are predicted proteins found by BLAST analysis of the Plant Gene Indices at The Institute for Genomic Research (TIGR) (http://www.tigr.org/

[1] Mention of trade names or commercial products in this publication is solely for the purpose of providing specific information and does not imply recommendation or endorsement by the United States Department of Agriculture.

[2] The nucleotide sequences described here have been deposited in the Genbank® database under the accession numbers AY819697 (*VfCBR1A* genomic clone), AY819698 (*VfCBR1B* mRNA), and AY819699 (*VfCBR1A* mRNA).

tdb/tgi/plant.shtml) representing CBR sequences from cotton (GmCBR2, EST assembly TC24661), maize (ZmCBR2, TC237132), *Medicago truncatula* (MtCBR2, TC79175), pepper (CaCBR2, TC413), rice (OsCBR1A, TC221002; OsCBR1B, TC233869; OsCBR2, TC225358), sorghum (SbCBR1A, TC91657; SbCBR1B, TC91540; SbCBR2, TC103004), soybean (GmCBR1A, TC192988; GmCBR1B, TC183655; GmCBR2, TC192958), tomato (LeCBR2, TC125368), and wheat (TaCBR1A, TC143609; TaCBR1B, TC165429; TaCBR2, TC152875).

2.3. Nucleic acid hybridization and gene expression analysis

The structure and genomic copy number of tung was analyzed by genomic Southern blotting, using non-radioactive digoxigenin-containing probes generated by PCR (PCR DIG Probe Synthesis Kit, Roche Applied Science, Indianapolis, IN). The genomic DNA sample lanes were flanked by lanes containing 15 ng of digoxigenin-labeled λ *Hin*dIII DNA (DNA Molecular Weight Marker II, Roche Applied Science). The membrane was prehybridized in DIG EasyHybe solution for 2–4 h at 50 °C, then hybridized in DIG EasyHybe containing 25 ng/ml of heat-denatured DIG-labeled PCR probe DNA overnight at 50 °C. The membranes were washed twice for 15 min with 2× SSC, 0.1% SDS at 50 °C, followed by three washes of 20 min each in 0.1× SSC, 0.1% SDS at 68 °C. Hybridizing fragments were detected by incubation with anti-DIG antibody, followed by chemiluminescent development with CDP-Star, and digital data capture and quantification using a Fuji LAS-1000Plus digital imaging system (Fuji Medical Systems, Stamford, CT).

Gene expression analysis was measured by semiquantitative RT-PCR [18,19]. Total RNA was extracted from tung leaves, flowers, and developing seeds by the hot borate method of Wan and Wilkins [20]. Equal quantities of RNA were reverse transcribed using the Superscript III First-Strand Synthesis System (Invitrogen). Equal volumes of each first strand reaction were amplified with gene-specific primer pairs. Aliquots of each sample were analyzed at various cycle numbers to determine the linear range of product synthesis. Expression levels were compared by agarose gel electrophoresis and visual estimation of ethidium bromide fluorescence intensity.

2.4. Transient transformation of tobacco cultured cells and immunofluorescence microscopy

Subcellular localization of various NADH:cytochrome b_5 reductases was determined by transient expression of myc-epitope-tagged versions of proteins in tobacco suspension cells, followed by comparisons of their resulting immunostaining patterns with the patterns attributable to endogenous organelle marker proteins [14]. Briefly, pRTL2 vectors (described earlier) harboring *CBR* cDNAs were biolistically bombarded into tobacco (*Nicotiana tabacum* cv. Bright Yellow 2) (BY-2) suspension-cultured cells, then cells were incubated at 26 °C for 20 h in covered Petri dishes to allow for gene expression and protein targeting. Cells were then fixed in formaldehyde and permeabilized with pectolyase Y-23 (Kyowa Chemical Products, Osaka, Japan) and Triton X-100 (Sigma-Aldrich Ltd., St. Louis, MO). For experiments designed to demonstrate the topological orientation of transiently expressed epitope-tagged CBR proteins, fixed and pectolyase-treated cells were differentially permeabilized with digitonin (25 μg/ml) (Sigma-Aldrich Ltd.), rather than Triton X-100, to perforate the plasma membrane but not organelle membranes [21].

Fixed, permeabilized cells were processed for indirect immunofluorescence microscopy as previously described [22]. Primary antibody sources and concentrations used were as follows: mouse anti-myc-epitope monoclonal antibody (1:100) (Princeton Monoclonal Antibody Facility); mouse anti-α-tubulin monoclonal antibody (1:500) (clone DM 1A; Sigma-Aldrich Ltd.); rabbit anti-E1β (1:1000) [23], rabbit anti-castor bean calreticulin (1:500) [24]. Fluorescent dye-conjugated secondary antibodies included goat anti-mouse Alexa Fluor 488 (1:1000); goat anti-rabbit Alexa Fluor 488 (1:1000) (Cedar Lane Laboratories Ltd.); goat anti-rabbit rhodamine red-X (1:500) (Jackson ImmunoResearch Laboratories Inc.). Concanavalin A conjugated to Alexa 594 was purchased from Molecular Probes (Eugene, OR) and incubated with BY-2 cells (1:200 dilution) during the final 20 min of the 60 min incubation with secondary antibodies.

Labeled cells were viewed using a Zeiss Axioskop 2 epifluorescence microscope (Carl Zeiss, Toronto, Canada) with a Zeiss 63X Plan Apochromat oil immersion objective (Carl Zeiss) and a Retiga 1300 CCD camera (Qimaging, Burnaby, Canada). All images shown were deconvolved and adjusted for brightness and contrast using Northern Eclipse 7.0 software (Empix Imaging, Mississauga, Canada), and then composed into figures using Adobe Photoshop 8.0 (Adobe Systems, San Jose, CA).

2.5. Yeast extract preparation and in vitro enzyme assay

CBR-pYES2.1 plasmids were transformed into wild-type yeast cells (strain SCY325 [25]) using the standard lithium acetate transformation protocol. Uracil prototrophs were grown in liquid media and cells harvested by centrifugation. The cell pellets were suspended in cell breaking buffer I [1× phosphate buffered saline containing dissolved Complete Mini EDTA-free protease cocktail tablets (Roche Applied Science, 1 tablet/10 ml buffer)] and lysed by vortexing in an equal volume of acid-washed 0.6 μm glass beads (4 × 1 min), followed by centrifugation at 1000 × *g* for 15 min to remove cellular debris and unbroken cells. The supernatants from the low-speed spin were used directly as enzyme sources. NADH:cytochrome b_5 reductase enzyme activity was quantified by measurement of Fe^{3+}-citrate

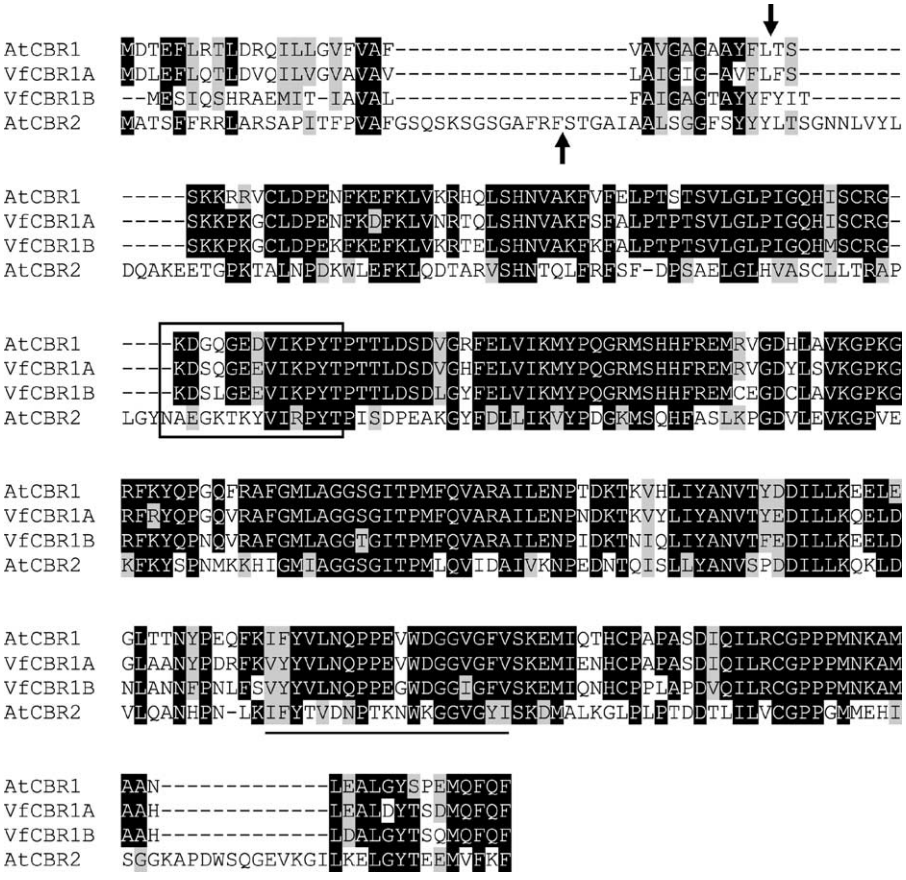

Fig. 1. Multiple sequence alignment of deduced amino acid sequences of VfCBR1A, VfCBR1B, AtCBR1 [7], and AtCBR2. Identical residues are shaded black, similar residues are shaded gray. The FAD binding site is boxed, and the NADH binding site is underlined. The down arrow denotes the end of the putative hydrophobic signal-anchor sequence for the type 1 enzymes, while the up arrow denotes the predicted cleavage site for the putative mitochondrial targeting peptide of AtCBR2.

reductase activity as described by Bagnaresi et al. [26]. Product formation was monitored continuously for 2 min at room temperature in an assay volume of 1 ml that contained 12.5 μg of total protein.

3. Results

3.1. Identification and cloning of tung CBR1A and CBR1B

Amplicons representing partial cDNAs for the 5′ ends of tung *CBR* were generated by PCR amplification from a preparation of developing tung seed cDNA library λ phage. Sequencing revealed the presence of two distinct cDNAs. Identification of the 3′ portions of these cDNAs was accomplished by 3′ RACE, followed by cloning of the full-length ORFs for both cDNAs. These cDNAs were named *VfCBR1A* and *VfCBR1B*, respectively. The predicted amino acid sequences of these two proteins are aligned with and compared to two CBR protein sequences from Arabidopsis (Fig. 1). Notably, there are only two *CBR* genes in the Arabidopsis genome, one of which encodes a microsomal-localized CBR protein [7], which we designate AtCBR1, and a second gene that encodes a putative CBR protein of unknown subcellular localization which we designate AtCBR2. The tung and Arabidopsis proteins exhibit a high degree of sequence similarity, and each of the proteins showed conserved features of the CBR protein family including NADH and FAD binding domains (Fig. 1). The most notable differences in the protein sequences were at the N-termini, which may be due to differences in protein localization signals. The N-termini of tung CBR1A, 1B, and AtCBR1, were similar to each other in that each protein contained a hydrophobic stretch of amino acids that was typical of an ER signal-anchor sequence. The AtCB5R2, however, contained a longer (approximately 25–30 amino acids) N-terminal sequence which was more amphipathic in nature and was not predicted to form a transmembrane domain, but rather exhibited the characteristics of a cleavable mitochondrial targeting peptide [27,28].

Phylogenetic analysis of tung and Arabidopsis CBR sequences with sequences of other known or putative CBR proteins confirmed that the two tung proteins were most closely related to AtCBR1 of Arabidopsis, while AtCBR2 was present in a distinctly different clade that was well-

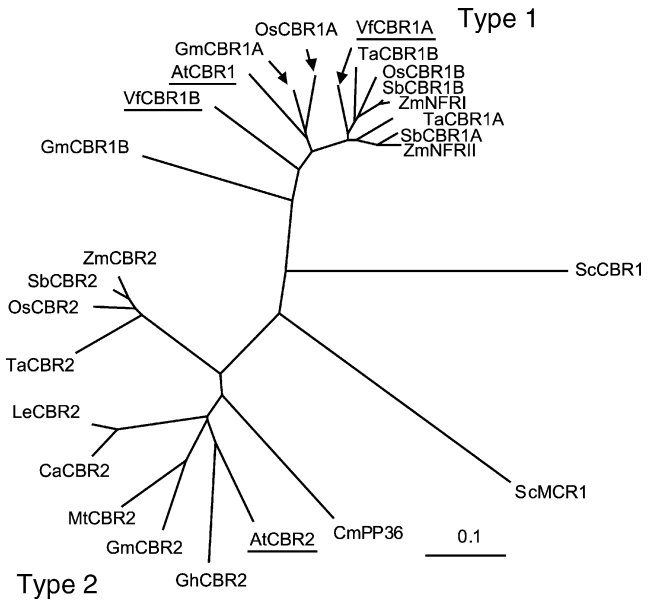

Fig. 2. Phylogenetic analysis of full-length CBR amino acid sequences from plants and *Saccharomyces cerevisiae*. The deduced amino acid sequences were aligned using CLUSTALX and displayed graphically with TreeView as described in the text. The branch lengths of the tree are proportional to divergence. The "0.1" scale represents 10% change. The sequences analyzed in this study are underlined. The Genbank® accession numbers for *VfCBR1A* and *VfCBR1B* are AY819699 and AY819698, respectively.

separated from the other type 1 enzymes (Fig. 2). Interestingly, the two *CBR* genes from yeast cells that encode either a microsomal (ScCBR1) or mitochondrial (ScMCR1) isoform of CBR proteins did not form a separate outgroup in the tree, but rather clustered closer towards the type 1 or type 2 CBR proteins in plants, respectively. These results suggest that plants, like yeast cells, contain at least two different types of CBR proteins, one representing microsomal-localized proteins (type 1), and the other mitochondrial proteins (type 2).

3.2. CBR gene structure and gene family size

The discovery of two *CBR1* genes from our initial PCR screening of the tung seed cDNA library, combined with the presence of at least four different cyt b_5 genes in tung [6], suggests that tung has evolved complex gene families for catalyzing electron transport pathways. To characterize the genomic organization of the tung *CBR* genes, we first isolated the gene sequences corresponding to *VfCBR1A* and *VfCBR1B* and compared their exon/intron structure to each other and to *AtCBR1* (Fig. 3). Quite surprisingly, the genomic structures of tung *CBR1A* and *1B* are considerably different. The *VfCBR1A* gene is made up of 9 exons and 8 introns, while *VfCBR1B* is intronless and is identical in size and structure to the 840 bp ORF of the *VfCBR1B* cDNA. Also surprising was the observation that the genomic structure, like the amino acid sequence, of *VfCBR1A* more

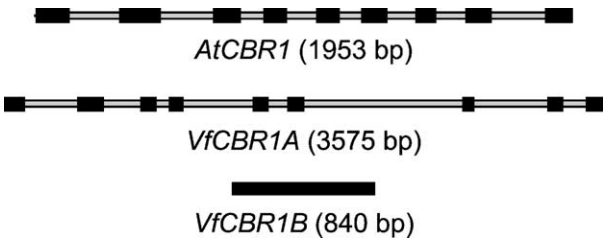

Fig. 3. Comparison of the genomic architecture of type 1 *CBR* genes from tung (*VfCBR1A* genomic clone, Genbank® accession AY819697) and Arabidopsis. The exon/intron junctions were determined by alignment of the open reading frame sequences with their respective genomic sequences. All exons (in black) and introns (in gray) are drawn to scale.

closely resembles *AtCBR1* (which is also made up of 9 exons and 8 introns) than it does the structure of *VfCBR1B*. The recovery of an intronless genomic PCR product for *VfCBR1B* was consistent; two different primer preparations and two different preparations of genomic DNA gave the same result.

The drastic differences between the structures of the two tung genes led us to investigate the possible existence of other uncloned *CBR* genes in tung. Southern blots were prepared from various restriction digests of tung genomic DNA and probed separately with the DIG-labeled ORFs for *VfCBR1A* and *VfCBR1B* (Fig. 4). The *VfCBR1A* probe hybridized to two *Hin*dIII bands and one *Xba*I band (lanes 1 and 2), which is consistent with a single *CBR1A* gene, given the absence of internal *Xba*I sites and the presence of a *Hin*dIII site at position 3068 of the 3575-bp genomic clone. The *VfCBR1B* probe, on the other hand, hybridized to three *Hin*dIII fragments (lane 4) and two *Xba*I fragments (lane 5), despite the absence of sites for either enzyme in the cloned *VfCBR1B* product, indicating the presence of additional

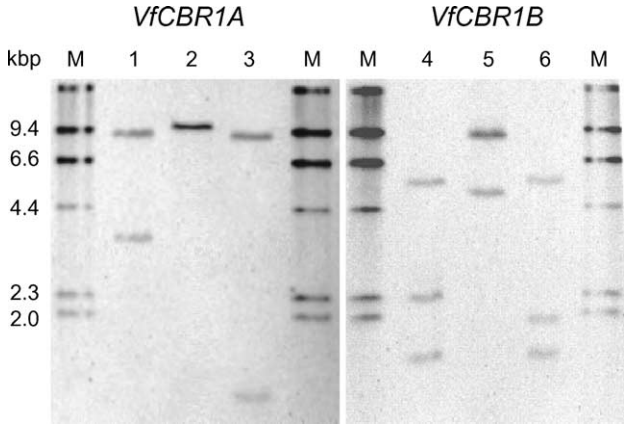

Fig. 4. Determination of type 1 CBR gene family size by Southern blot hybridization analysis of tung genomic DNA probed with DIG-labeled full-length ORF for *VfCBR1A* or *VfCBR1B*. Twenty-five micrograms of genomic DNA was digested with *Hin*dIII (lanes 1 and 4), *Xba*I (lanes 2 and 5) or both *Hin*dIII and *Xba*I (lanes 3 and 6), transferred to nylon membrane, then probed and analyzed as described in the text. M = DIG-labeled λ *Hin*dIII DNA size standard.

genes related to *VfCBR1B*. Probing additional Southern blots of tung genomic DNA cut with other combinations of restriction enzymes suggested that both of the additional bands in lane 4 of Fig. 4 come from a single gene (data not shown).

While it is likely that tung also contains a type 2 CBR gene, we were unable to detect a corresponding cDNA in our tung seed library by PCR-based screening, nor were we able to identify a genomic fragment by anchor-adapted PCR. Since the type 2 enzyme likely represents a putative mitochondrial isoform, and we are interested primarily in metabolic events in the ER, we did not pursue the identification of a type 2 enzyme any further.

3.3. Gene expression analysis

Most of the existing plant CBR literature indicates that *CBR* genes are expressed rather widely, if not constitutively, in most plant organs tested [7,12,13]. Given the apparent complexity of the cyt b_5 and *CBR* gene families in tung, and our ongoing interest in seed oil biosynthesis, we analyzed the organ-specific expression patterns of *VfCBR1A* and *VfCBR1B* to look for suggestions of functional specialization between the two genes through differences in gene expression profiles. The full-length ORF probes used for genomic analysis, though specific on Southern blots, cross-hybridized to each other on northern blots (data not shown) so gene expression was estimated by semiquantitative RT-PCR using gene-specific primer pairs. Total RNA per RT reaction, first strand reaction per PCR reaction, and PCR cycle number were equal for all samples. The tung *Actin2* gene was used as a control. Control samples generated without reverse transcriptase confirmed that all samples were free of genomic DNA contamination. Both *VfCBR* genes are expressed in tung leaves, flowers, and developing seeds at approximately similar levels (Fig. 5). The overlapping expression patterns suggest redundant functions for the two enzymes.

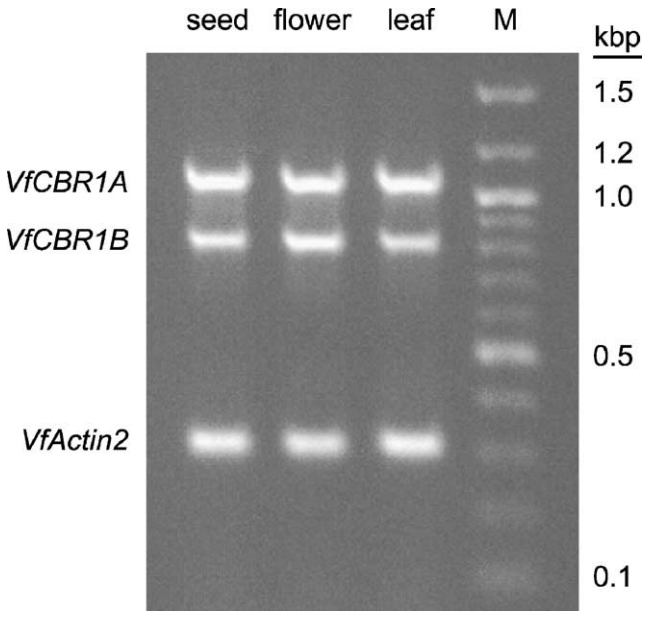

Fig. 5. RNA expression analysis of *VfCBR1A* and *VfCBR1B*. Gene-specific primer pairs were used to analyze the relative expression levels in tung leaves, flowers, and developing seeds by semiquantitative RT-PCR, as described in the text. The tung *Actin2* gene was used as a control. M = 100 bp marker (New England Biolabs).

3.4. Subcellular localization and topology mapping of CBR proteins

To determine the subcellular localization of the tung CBR proteins, and also to determine whether the second clade of proteins present in the phylogram of Fig. 2 does indeed

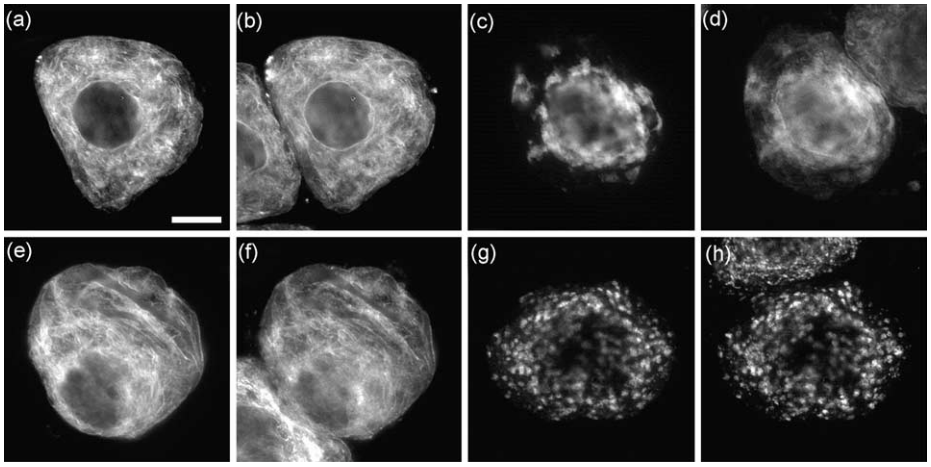

Fig. 6. Immunolocalization of plant CBR proteins in tobacco BY-2 cells. BY-2 cells were transiently transformed with individual myc-tagged CBR proteins and processed for indirect immunofluorescence microscropy (see Section 2 for details). Colocalization of the immunostaining patterns attributable to either introduced VfCBR1A (a), VfCBR1B (c), or AtCBR1 (e) and the ER stain concanavalin A (b, d and f) in the same cells. Note the presence of concanavalin-stained ER in adjacent non-transformed cells (b, d and f). Colocalization of the immunostaining patterns attributable to AtCBR2 (g) and endogenous mitochondrial E1β (h) in the same cell. Bar in (a) = 10 μm.

represent mitochondrial localized isoforms of CBR (as predicted by bioinformatics methods), we characterized the subcellular localization of VfCBR1A, VfCBR1B, AtCBR1, and AtCBR2 proteins. Each CBR protein was epitope-tagged at the C-terminus, followed by transient expression of the plasmids in tobacco BY-2 suspension cells and processing for indirect immunofluorescence microscopy. The myc-epitope tag sequence was added to the C-terminus of the proteins rather than N-terminus, since the putative microsomal or mitochondrial localization signals were present within the N-terminal regions. Addition of an epitope tag also provided a monospecific epitope that allowed us to distinguish between the transiently expressed CBR proteins and endogenous CBR proteins within BY-2 cells. Inspection of the immunofluorescence staining patterns of VfCBR1A, VfCBR1B, and AtCBR1 revealed that they were identical to the staining pattern for dye-conjugated concanavalin A, a marker stain for the ER

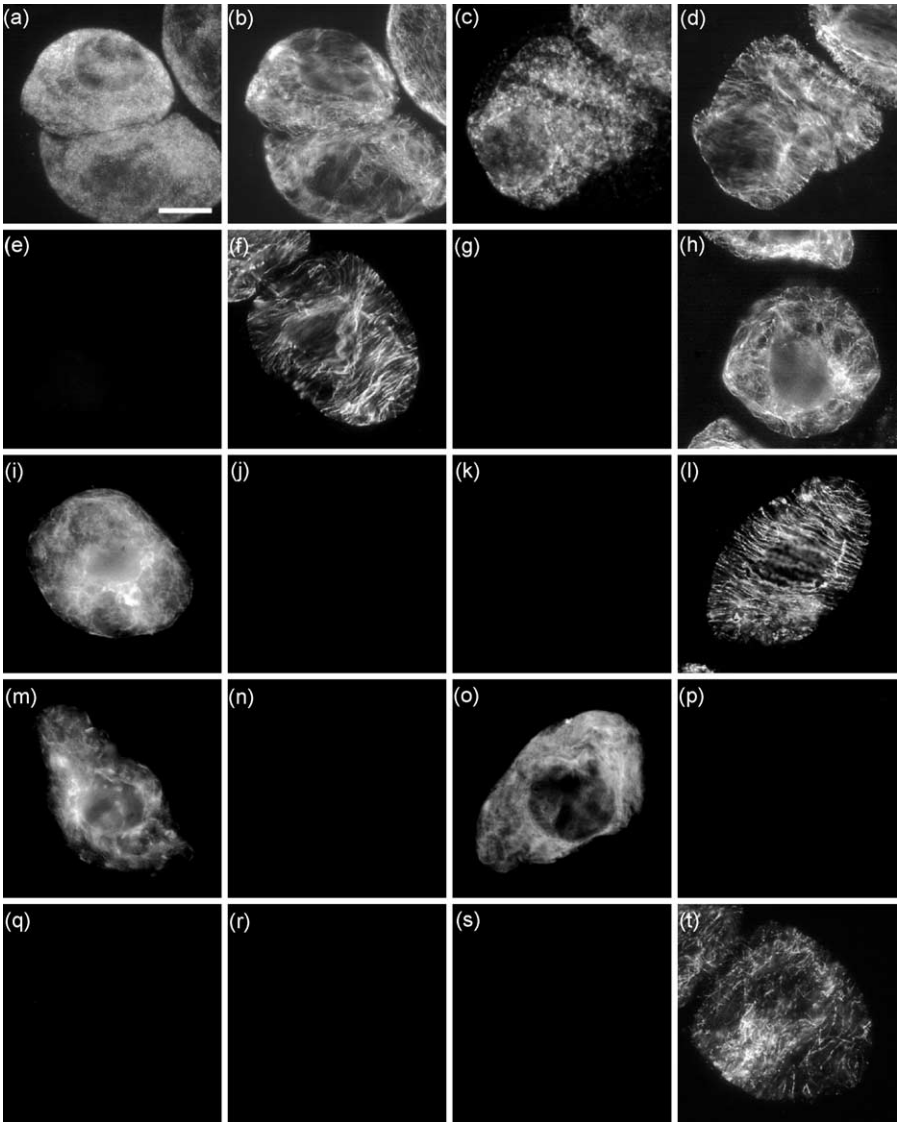

Fig. 7. Topological mapping of plant CBR proteins in tobacco BY-2 cells. The presence or absence of immunofluorescence illustrates the membrane topology of transiently expressed epitope-tagged CBR proteins in differential-permeabilized tobacco BY-2 cells. Non-transformed (a–h) or transiently transformed (i–t) cells were fixed and permeabilized using either Triton X-100 (a–d), which perforates all cellular membranes, or digitonin (e–t), which selectively permeabilizes the plasma membranes, then cells were processed for immunofluorescence microscopy. Immunostaining of endogenous calreticulin in the lumen of the ER (a), endogenous E1β in the mitochondrial matrix (c) and tubulin in cytosolic microtubules (b and d) in the same non-transformed, Triton X-100-permeabilized cells. Lack of immunostaining of endogenous calreticulin (e) or E1β (g) but the presence of cytosolic tubulin (f and h) in the same digitonin-permeabilized cells. Immunostaining of expressed C-terminal myc-VfCBR1A (i), but absence of endogenous ER calreticulin (j) staining in the same digitonin-permeabilized cells. Lack of immunostaining of N-terminal myc-VfCBR1A (k), but the presence of endogenous tubulin (l) in the same digitonin-permeabilized cells. Immunostaining of C-terminal myc-VfCBR1B (m) and C-terminal myc-AtCBR1 (o) in the ER, but absence of endogenous ER calreticulin (n and p) staining in the same digitonin-permeabilized cells. Lack of immunostaining of C-terminal myc-AtCBR2 (q and s) and endogenous E1β staining (r), but the presence of cytosolic tubulin (t) in the same digitonin-permeabilized cells. Bar in (a) = 10 μm.

(Fig. 6a–f). The aggregation of ER membranes caused by VfCBR1B (Fig. 6c and d) may be due to overexpression of the protein, which is often observed when overexpressing certain ER localized membrane-bound enzymes in BY-2 cells [4]. The staining pattern for AtCBR2 did not colocalize with concanavalin A (data not shown), however, but rather was identical to the staining pattern of E1β (Fig. 6g and h), which is a marker protein for the mitochondrial matrix. Collectively, these data indicate that VfCBR1A, VfCBR1B, and AtCBR1 are localized to the ER while AtCBR2 is located in mitochondria.

To investigate the topological orientation of CBR proteins in membranes, tobacco BY-2 cells were transiently transformed with the CBR constructs, then cells were fixed and treated with either Triton X-100 or digitonin to selectively permeabilize cellular membranes. Incubation of cells with Triton X-100 perforates all cellular membranes, allowing immunodetection of epitopes located within subcellular compartments (e.g., calreticulin in the ER lumen, Fig. 7a, or E1β in the mitochondrial matrix, Fig. 7c) or the cytosol (tubulin – Fig. 7b and d). Incubation of cells with digitonin, however, perforates the plasma membrane only, allowing immunodetection of cytosolic-exposed (tubulin, Fig. 7f and h), but not organelle protected epitopes (e.g., calreticulin in the ER lumen, Fig. 7e, or E1β in the mitochondrial matrix, Fig. 7g). Incubation of transiently transformed BY-2 cells with digitonin resulted in immunodetection of C-terminally tagged VfCBR1A (Fig. 7i), VfCBR1B (Fig. 7m), and AtCBR1 (Fig. 7o), but not the ER lumen marker protein calreticulin (Fig. 7j, n, and p), indicating that the C-terminus of each CBR protein was located on the cytosolic side of ER membranes. The C-terminally tagged AtCBR2 protein was not detected in digitonin-permeabilized cells (Fig. 7q and s), suggesting that the predicted N-terminal mitochondrial presequence directed import into the protein into the mitochondrial matrix. Addition of a myc-epitope tag sequence to the N-terminus of the ER-localized CBR isoforms (VfCBR1A, VfCBR1B, and AtCBR1), followed by transient expression and treatment of cells with Triton X-100, confirmed that each of these proteins was still localized to the ER (by virtue of colocalization with the ER marker protein; data not shown), but the N-terminal epitope tag was not immunodetectable in digitonin treated cells, while the cytosolic marker protein tubulin was (data shown only for VfCBR1A; Fig. 7k and l). These results indicate that the ER-localized CBR proteins are type I membrane proteins that are anchored to the membrane with the N-terminus in the lumen, and the majority of the protein, including the C-terminus and catalytic domain, located on the cytosolic side of the membrane.

3.5. Yeast overexpression and in vitro CBR enzyme assay

To characterize the enzyme activity of the ER-localized CBR proteins, each cDNA was cloned into the *S. cerevisiae* expression vector pYES2.1-V5HisTOPO (high-copy, *URA*) and transformed into the wild-type yeast strain SCY325 [25]. Cell-free extracts were used to test for reductase activity, as measured by the ability to reduce Fe^{+3}-citrate, a typical iron chelate acted upon by many cyt b_5 reductases [13]. Results presented in Fig. 8 demonstrate that both AtCBR1 and VfCBR1A were active under the given assay conditions, respectively producing 11- and 20-fold more Fe-dye complex than the empty vector control. However, VfCBR1B was not active, possibly reflecting an inability of this enzyme to reduce the specific iron chelate used in the assay. Western blot analysis of yeast lysates expressing C-terminal myc-epitope-tagged CBR proteins indicated that AtCBR1, VfCBR1A, and VfCBR1B were all expressed at approximately equal levels (data not shown). These results suggested that neither large differences in protein expression levels nor instability of VfCBR1B acccounted for the lack of activity of VfCBR1B in our assays. The extremely low level of endogenous activity observed in the empty vector control assays is probably attributable to the short duration of the assay and the small quantities of protein used (see Section 2.5). Both AtCBR1 and VfCBR1A were unable to utilize NADPH as an electron donor, consistent with the findings for the cloned Arabidopsis enzyme (Fig. 8 and [7]), thus reinforcing the hypothesis that this family of enzymes displays strict specificity for NADH.

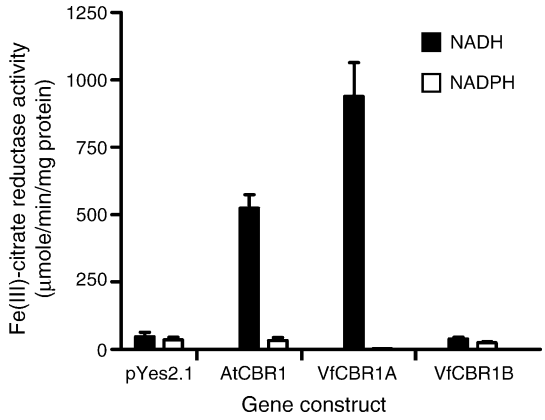

Fig. 8. Measurement of in vitro enzyme activity by type 1 CBR proteins. Galactose-inducible yeast expression constructs for VfCBR1A, VfCBR1B, and AtCBR1 were transformed into wild-type *S. cerevisiae*. Cell-free lysates were prepared from induced cultures and used to measure enzyme activity of the overexpressed proteins as a function of their ability to reduce Fe^{3+}-citrate [12], and compared to activity from the negative control strain carrying a vector with no insert. NADH (black bars) or NADPH (white bars) was supplied as reductant. Measurements were performed in triplicate and the error bars represent the standard deviations.

4. Discussion

Production of industrially useful oils in transgenic oilseeds has proven to be a formidable challenge. Many labs have addressed the issue, and much progress has been made. However, the levels of novel fatty acid produced in transgenic crops very often still fall far below the levels

observed in the triacylglycerol fraction of the native species [1]. The initial discoveries of the acyl-ACP thioesterases and FAD2-like desaturases and conjugases that directly synthesize the novel fatty acids provided the fundamental tools needed to drive this field forward. However, it has become abundantly clear that these genes alone are not sufficient to meet the ultimate goal. Therefore, the research has shifted toward finding and characterizing other enzymes in the native plant that are necessary for efficient packaging and storage of the target fatty acid in triacylglycerol.

With good reason, the new targets most often have been the various CoA-dependent and CoA-independent acyltransferases that collectively channel fatty acids away from phospholipids toward triacylglycerols [29–37]. While this class of genes is also of interest to us, we considered the possibility that the host organism acyltransferases might not be the only enzymes that are insufficient to drive high-level novel fatty acid accumulation. The enzymes that make up the electron transport chain that supplies reduced electrons to FADX during eleostearic acid biosynthesis could also be limiting factors. Other reports have shown that specific isoforms of the cofactor protein acyl carrier protein (ACP) and the plastidial electron donor ferredoxin can increase unusual fatty acid synthesis [38,39], so we sought to learn more about the electron transport chain proteins present in developing tung seed. Recently, this laboratory cloned and characterized four isoforms of cytochrome b_5 [6]. In this report, we have presented information about two isoforms of NADH:cytochrome b_5 reductase.

Neither gene is dedicated to eleostearic acid biosynthesis; both are expressed in leaves, flowers, and developing seeds (Fig. 5). It is likely, though, that other *CBR* genes might also be expressed in tung seeds and/or other tung organs as well. Genomic southern blotting revealed at least one additional gene related to *VfCBR1B*. This additional *CBR1B* gene has not been cloned; however, it is tempting to speculate that it may be the more anciently conserved relative to *CBR1A*, and that its intron/exon structure would more closely resemble that of *CBR1A* than does the intronless *CBR1B* gene cloned in this study. How the cloned *CBR1B* gene came to exist is purely a matter of speculation, but the intronless structure would suggest synthesis and chromosomal reintegration of a double-stranded product from the ancient *VfCBR1B* mRNA, perhaps initiated through reverse transcription.

Both tung isoforms described here share strong sequence similarity to CBR1 of Arabidopsis. Immunofluorescence studies demonstrated that tung CBR1A, CBR1B, and Arabidopsis CBR1 are targeted to the ER, which is consistent with the biochemical data for AtCBR1 [7], and supports the hypothesis that these isoforms may play a role in fatty acid desaturation/conjugation reactions in the ER of developing tung seeds. Based on the data from Fig. 6, it is tempting to speculate the all type 1 CBR enzymes are targeted to the ER. The maize proteins NFRI and NFRII, however, are putatively targeted to the tonoplast [13], despite sitting firmly in the midst of the type 1 clade of the phylogenetic tree in Fig. 2. The cause of this apparent discrepancy between targeting and phylogeny is not known at this time. Characterization and subcellular localization of other type 1 enzymes, especially those very close to NFRI and NFRII in Fig. 2, may help to resolve this issue.

However, fatty acid biosynthesis is not confined to the ER. Mitochondria also possess the machinery to manufacture fatty acids [40], and recent reports from plants indicate the presence of cytochrome b_5-containing electron transport chains in this compartment. Tung seeds express at least four cytochrome b_5 genes, and one of these is clearly targeted to mitochondria [6]. In addition to the ER-localized reductase activities, a mitochondrial isoform of CBR has been characterized in yeast [16,17] and a mitochondrial isoform (AtCBR2, Fig. 2) is also present in Arabidopsis. In fact, most of the type 2 proteins compared in Fig. 2 are likely targeted to mitochondria. A possible exception is the extracellular protein CmPP36. This protein was discovered in the phloem sap of *Cucurbita maxima*, and is thought to help regulate the cellular supply of reduced iron during periods of iron deprivation [15]. The soluble extracellular form of CmPP36 appears to be a processed form of a larger, membrane-bound preprotein [15]. The full-length form of this protein gives a very strong mitochondrial targeting score (0.925, reliability class = 1) when analyzed by the TargetP program [28], and notably, this N-terminal sequence is absent from the mature protein found in the phloem exudate. It is therefore possible that the signal sequence of CmPP36 could recently have evolved from a cleavable mitochondrial targeting sequence, thus explaining the otherwise strong phylogenetic relationship between this protein and the other members of the type 2 group. Alternatively, there may be as yet uncharacterized biogenetic relationships between mitochondrial proteins and proteins found in the phloem exudate. In yeast cells, the single mitochondrial CBR protein is localized to both the intermembrane space and the outer membrane, and this dual localization has been attributed to the incomplete translocation of the targeting peptide into mitochondria [15]. Partial translocation results in partitioning of the protein into the mitochondrial outer membrane, while more complete translocation results in cleavage of the targeting peptide and release of the protein into the intermembrane space. Perhaps some plant mitochondrial CBR proteins are initially tethered to the mitochondrial outer membrane by the N-terminal anchor sequence, then proteolytically cleaved to generate a soluble protein for release into the phloem. Our data for Arabidopsis CBR2, however, suggest that this protein is completely translocated into the mitochondrial matrix. Additional experiments using homologous proteins in specific tissues or organs will be required to resolve these issues. Although uncharacterized at this point, it is likely that tung also contains type 2 *CBR* genes. The widespread occurrence of type 2 *CBR* sequences in many plant species (Fig. 2), and the presence of distinct mitochondrial and ER CBR proteins in yeast cells that

group with these two families of plant sequences, suggests that the divergence of the ancestral *CBR* gene into ER- and mitochondrial-targeted gene families was a relatively ancient evolutionary event.

Acknowledgements

We thank Sean Coughlan and Jan Miernyk for providing antibodies, and Steven Sturley for providing the yeast strain SCY325. We also thank Rae Kuan and Kevin Gipson (USDA-ARS-SRRC) for excellent technical assistance. This work was supported by the United States Department of Agriculture, Agricultural Research Service (Current Research Information System project number 6435-41000-083D to J.M.S., D.C.C., and J.M.D.), the Louisiana Board of Regents, Governor's Biotechnology Initiative (J.M.D. and T.D.), and the Natural Sciences and Engineering Research Council (grant no. 217291) and Ontario Premier's Research in Excellence Award to R.T.M.

Appendix A. Supplementary data

Supplementary data associated with this article can be found, in the online version, at doi:10.1016/j.plantsci.2005.03.023.

References

[1] J.J. Thelen, J.B. Ohlrogge, Metabolic engineering of fatty acid biosynthesis in plants, Metab. Eng. 4 (2002) 12–21.
[2] J. Shanklin, E.B. Cahoon, Desaturation and related modifications of fatty acids, Annu. Rev. Plant Physiol. Plant Mol. Biol. 49 (1998) 611–641.
[3] D.S. Knutzon, T.R. Hayes, A. Wyrick, H. Xiong, H. Maelor Davies, T.A. Voelker, Lysophosphatidic acid acyltransferase from coconut endosperm mediates the insertion of laurate at the sn-2 position of triacylglycerols in lauric rapeseed oil and can increase total laurate levels, Plant Physiol. 120 (1999) 739–746.
[4] J.M. Dyer, D.C. Chapital, J.C. Kuan, R.T. Mullen, C. Turner, T.A. McKeon, A.B. Pepperman, Molecular analysis of a bifunctional fatty acid conjugase/desaturase from tung. Implications for the evolution of plant fatty acid diversity, Plant Physiol. 130 (2002) 2027–2038.
[5] J.M. Dyer, D.C. Chapital, J.C. Kuan, H.S. Shepherd, F. Tang, A.B. Pepperman, Production of linoleic acid in yeast cells expressing an omega-3 desaturase from tung (*Aleurites fordii*), J. Am. Oil Chem. Soc. 81 (2004) 647–651.
[6] Y.T. Hwang, S.M. Pelitire, M.P. Henderson, D.W. Andrews, J.M. Dyer, R.T. Mullen, Novel targeting signals mediate the sorting of different isoforms of the tail-anchored membrane protein cytochrome b_5 to either endoplasmic reticulum or mitochondria, Plant Cell 16 (2004) 3002–3019.
[7] M. Fukuchi-Mizutani, M. Mizutani, Y. Tanaka, T. Kusumi, D. Ohta, Microsomal electron transfer in higher plants: cloning and heterologous expression of NADH-cytochrome b_5 reductase from *Arabidopsis*, Plant Physiol. 119 (1999) 353–362.
[8] M.A. Smith, L. Jonsson, S. Stymne, K. Stobart, Evidence for cytochrome b_5 as an electron donor in ricinoleic acid biosynthesis in microsomal preparations from developing castor bean (*Ricinus communis* L.), Biochem. J. 287 (1992) 141–144.
[9] S.F. Altschul, T.L. Madden, A.A. Schaffer, J. Zhang, Z. Zhang, W. Miller, D.J. Lipman, Gapped BLAST and PSI-BLAST: a new generation of protein database search programs, Nucl. Acids Res. 25 (1997) 3389–3402.
[10] N. Saitou, M. Nei, The neighbor-joining method: a new method for reconstructing phylogenetic trees, Mol. Biol. Evol. 4 (1987) 406–425.
[11] R.D. Page, TreeView: an application to display phylogenetic trees on personal computers, Comput. Appl. Biosci. 12 (1996) 357–358.
[12] P. Bagnaresi, S. Thoiron, M. Mansion, M. Rossignol, P. Pupillo, J.F. Briat, Cloning and characterization of a maize cytochrome-b_5 reductase with Fe^{3+}-chelate reduction capability, Biochem. J. 338 (1999) 499–505.
[13] P. Bagnaresi, D. Mazars-Marty, P. Pupillo, F. Marty, J.F. Briat, Tonoplast subcellular localization of maize cytochrome b_5 reductases, Plant J. 24 (2000) 645–654.
[14] J.M. Dyer, R.T. Mullen, Immunocytological localization of two plant fatty acid desaturases in the endoplasmic reticulum, FEBS Lett. 494 (2001) 44–47.
[15] B. Xoconostle-Cazares, R. Ruiz-Medrano, W.J. Lucas, Proteolytic processing of CmPP36, a protein from the cytochrome b(5) reductase family, is required for entry into the phloem translocation pathway, Plant J. 24 (2000) 735–747.
[16] K. Hahne, V. Haucke, L. Ramage, G. Schatz, Incomplete arrest in the outer membrane sorts NADH-cytochrome b_5 reductase to two different submitochondrial compartments, Cell 79 (1994) 829–839.
[17] M. Csukai, M. Murray, E. Orr, Isolation and complete sequence of CBR, a gene encoding a putative cytochrome *b* reductase in *Saccharomyces cerevisiae*, Eur. J. Biochem. 219 (1994) 441–448.
[18] J.M. Shockey, M.S. Fulda, J. Browse, *Arabidopsis* contains a large superfamily of acyl-activating enzymes. Phylogenetic and biochemical analysis reveals a new class of acyl-coenzyme a synthetases, Plant Physiol. 132 (2003) 1065–1076.
[19] J.M. Shockey, M.S. Fulda, J.A. Browse, *Arabidopsis* contains nine long-chain acyl-coenzyme a synthetase genes that participate in fatty acid and glycerolipid metabolism, Plant Physiol. 129 (2002) 1710–1722.
[20] C.Y. Wan, T.A. Wilkins, A modified hot borate method significantly enhances the yield of high-quality RNA from cotton (*Gossypium hirsutum* L.), Anal. Biochem. 223 (1994) 7–12.
[21] R.T. Mullen, C.S. Lisenbee, C.R. Flynn, R.N. Trelease, Stable and transient expression of chimeric peroxisomal membrane proteins induces an independent "zippering" of peroxisomes and an endoplasmic reticulum subdomain, Planta 213 (2001) 849–863.
[22] R.N. Trelease, M.S. Lee, A. Banjoko, J. Bunkelmann, C-terminal polypeptides are necessary and sufficient for in-vivo targeting of transiently-expressed proteins to peroxisomes in suspension-cultured cells, Protoplasma 195 (1996) 156–167.
[23] M.H. Luethy, N.R. David, T.E. Elthon, J.A. Miernyk, D.D. Randall, Characterization of a monoclonal antibody directed against the E1a subunit of plant pyruvate dehydrogenase, J. Plant Physiol. 145 (1995) 442–449.
[24] S.J. Coughlan, C. Hastings, R. Winfrey Jr., Cloning and characterization of the calreticulin gene from *Ricinus communis* L., Plant Mol. Biol. 34 (1997) 897–911.
[25] P. Oelkers, D. Cromley, M. Padamsee, J.T. Billheimer, S.L. Sturley, The DGA1 gene determines a second triglyceride synthetic pathway in yeast, J. Biol. Chem. 277 (2002) 8877–8881.
[26] P. Bagnaresi, B. Basso, P. Pupillo, The NADH-dependent Fe(3+)-chelate reductases of tomato roots, Planta 202 (1997) 427–434.
[27] K. Nakai, P. Horton, PSORT: a program for detecting sorting signals in proteins and predicting their subcellular localization, Trends Biochem. Sci. 24 (1999) 34–36.
[28] O. Emanuelsson, H. Nielsen, S. Brunak, G. von Heijne, Predicting subcellular localization of proteins based on their N-terminal amino acid sequence, J. Mol. Biol. 300 (2000) 1005–1016.
[29] A.P. Brown, S. Carnaby, C. Brough, M. Brazier, A.R. Slabas, *Limnanthes douglasii* lysophosphatidic acid acyltransferases: immunolo-

gical quantification, acyl selectivity and functional replacement of the *Escherichia coli* plsC gene, Biochem. J. 364 (2002) 795–805.
[30] D.H. Hobbs, C. Lu, M.J. Hills, Cloning of a cDNA encoding diacylglycerol acyltransferase from *Arabidopsis thaliana* and its functional expression, FEBS Lett. 452 (1999) 145–149.
[31] D.S. Knutzon, K.D. Lardizabal, J.S. Nelsen, J.L. Bleibaum, H.M. Davies, J.G. Metz, Cloning of a coconut endosperm cDNA encoding a 1-acyl-sn-glycerol-3-phosphate acyltransferase that accepts medium-chain-length substrates, Plant Physiol. 109 (1995) 999–1006.
[32] U. Stahl, A.S. Carlsson, M. Lenman, A. Dahlqvist, B. Huang, W. Banas, A. Banas, S. Stymne, Cloning and functional characterization of a phospholipid:diacylglycerol acyltransferase from *Arabidopsis*, Plant Physiol. 135 (2004) 1324–1335.
[33] Z. Zheng, Q. Xia, M. Dauk, W. Shen, G. Selvaraj, J. Zou, Arabidopsis AtGPAT1, a member of the membrane-bound glycerol-3-phosphate acyltransferase gene family, is essential for tapetum differentiation and male fertility, Plant Cell 15 (2003) 1872–1887.
[34] C. Hanke, F.P. Wolter, J. Coleman, G. Peterek, M. Frentzen, A plant acyltransferase involved in triacylglycerol biosynthesis complements an *Escherichia coli* sn-1-acylglycerol-3-phosphate acyltransferase mutant, Eur. J. Biochem. 232 (1995) 806–810.
[35] M.W. Lassner, C.K. Levering, H.M. Davies, D.S. Knutzon, Lysophosphatidic acid acyltransferase from meadowfoam mediates insertion of erucic acid at the sn-2 position of triacylglycerol in transgenic rapeseed oil, Plant Physiol. 109 (1995) 1389–1394.
[36] X. He, C. Turner, G.Q. Chen, J.T. Lin, T.A. McKeon, Cloning and characterization of a cDNA encoding diacylglycerol acyltransferase from castor bean, Lipids 39 (2004) 311–318.
[37] K.D. Lardizabal, J.T. Mai, N.W. Wagner, A. Wyrick, T. Voelker, D.J. Hawkins, DGAT2 is a new diacylglycerol acyltransferase gene family: purification, cloning, and expression in insect cells of two polypeptides from *Mortierella ramanniana* with diacylglycerol acyltransferase activity, J. Biol. Chem. 276 (2001) 38862–38869.
[38] D.J. Schultz, M.C. Suh, J.B. Ohlrogge, Stearoyl-acyl carrier protein and unusual acyl-acyl carrier protein desaturase activities are differentially influenced by ferredoxin, Plant Physiol. 124 (2000) 681–692.
[39] M.C. Suh, D.J. Schultz, J.B. Ohlrogge, Isoforms of acyl carrier protein involved in seed-specific fatty acid synthesis, Plant J. 17 (1999) 679–688.
[40] H. Wada, D. Shintani, J. Ohlrogge, Why do mitochondria synthesize fatty acids? Evidence for involvement in lipoic acid production, Proc. Natl. Acad. Sci. U.S.A. 94 (1997) 1591–1596.